SUPPLEMENTAL MATERIAL

ARTICLE HISTORY
Compiled December 6, 2022

Notations and outline

We describe the notation that we will use throughout the paper. We use regular lowercase letters for scalars, **bold lowercase letters** for vectors, **BOLD CAPITAL LETTERS** for matrices, and normal CAPITAL LETTERS for sets. We use subscript i for i-th element. Superscript represents iteration steps (k for outer iteration and j for inner loop). For a vector $\boldsymbol{v}$, $\|\boldsymbol{v}\|_{l_0}$, $\|\boldsymbol{v}\|_{l_2}$, and $\|\boldsymbol{v}\|_{l_\infty}$ denote l_0-, l_2-, and l_∞-norms, respectively. $\text{supp}(\boldsymbol{v})$ represents the nonzero elements of $\boldsymbol{v}$. For a vector $\boldsymbol{v} \in \mathbb{R}^n$, $\boldsymbol{u} = \max\{\boldsymbol{v}, \mathbf{0}\}$ denotes $u_i = \max\{v_i, 0\}$, $i = 1, 2, \cdots, n$. The space $\mathbb{R}^n_+$ stands for $\{\boldsymbol{v} \in \mathbb{R}^n : \ \boldsymbol{v} \geq \mathbf{0}\}$. For a matrix $\mathbf{\Phi} \in \mathbb{R}^{m\times n}$ and an index set $\mathrm{A} \subseteq \{1, 2, \cdots, n\}$, $\mathbf{\Phi}_\mathrm{A}$ stands for the submatrix of $\mathbf{\Phi}$ obtained by keeping only the columns indexed by A. Also, $\boldsymbol{v}_\mathrm{A}$ denotes the vector obtained by keeping only the components of a vector $\boldsymbol{v} \in \mathbb{R}^n$ indexed by A.

Comparsion between l_0 and l_1 norm

To promote sparsity of the target signals and images, recent studies show that non-convex approximations of the l_0-norm are more efficient, and the nonconvex penalties usually have better performances than l_1 penalty [1,2]. This is because the l_1 regularized model induces bias for large coefficients [3]. Further, when l_1-norm is considered, the solver to the problem has to be carefully designed and usually not sufficiently efficient. For l_0-norm optimization problems, despite the NP-hardness, lots of efficient solvers have been introduced, and most of the approaches are threshold-based algorithms, e.g., IHT [4], OMP [5], CoSaMP [6], HTP [7] and so on. All above mentioned algorithms are efficient and performs well in compressed sensing problems[8] but rely on a properly estimation of the sparsity level. However, in our treatment planning optimization problem, the sparsity level may vary in different cases and is not easy to estimate.

Table 1. Two clinical cases for evaluation

Disease set	Start beam angle (deg)	End beam angle (deg)	Number of control points	Spot number at 0 sparsity
Intracranial	1.3	96.3	37	4934
Lung	322.5	197.5	44	9808

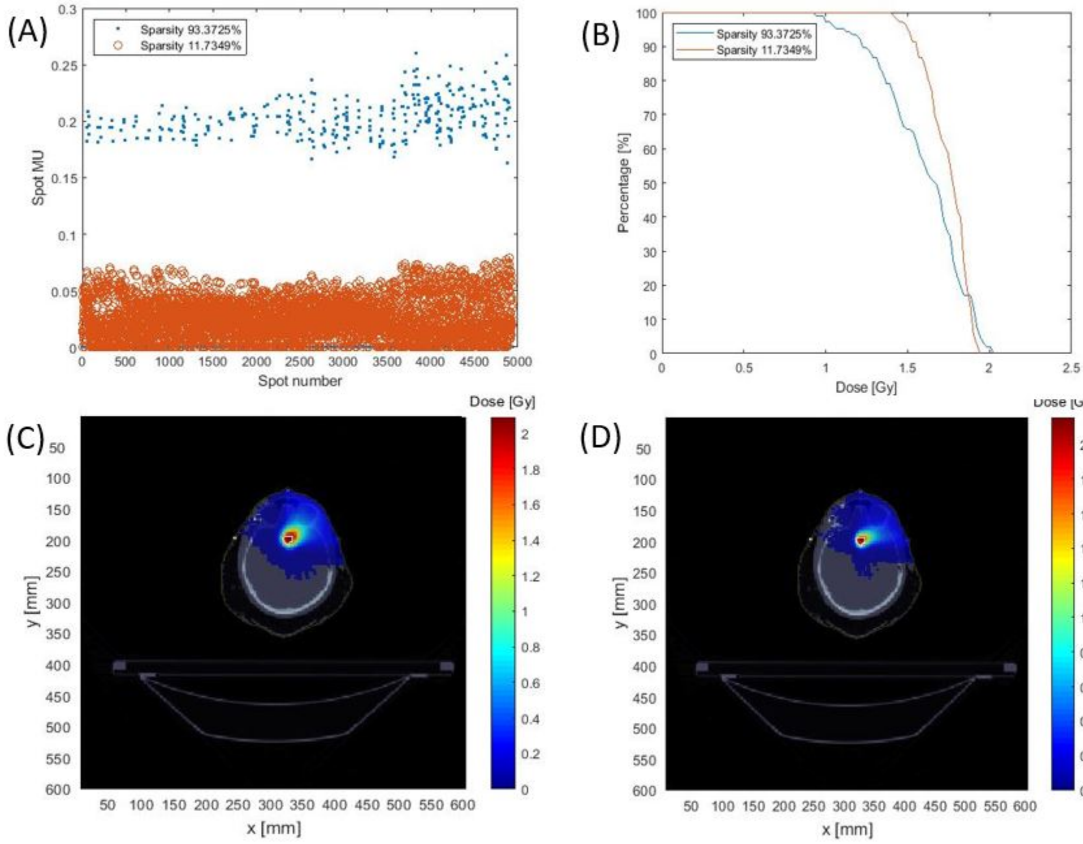

Figure 1. Comparison between high sparsity and low sparsity in an intracranial target brain case .The prescription dose is 54Gy and 1.8Gy per fraction. (A) High sparsity resulted in a higher averaged spot MU. (B) Dose-volume histogram (DVH) per fraction shows low sparsity has better plan quality. (C) Dose distribution for 11.7% sparsity. (D) Dose distribution for 93.4% sparsity.

Computation complexity analysis

If it holds $\boldsymbol{p}_0 = \boldsymbol{\Phi}\boldsymbol{w}^\star + \boldsymbol{p}_\varepsilon$ for some sparse vector $\boldsymbol{w}^\star$ and sufficiently small $\boldsymbol{\varepsilon}$ such that $\|\boldsymbol{p}_\varepsilon\|_{l_2} \leq \varepsilon$, then under certain assumptions on the fluence matrix, e.g. restricted isometry property (RIP) [9], mutual incoherence property (MIP) [10], the support of the minimizer will coincide with that of the true signal $\boldsymbol{w}^\star$ if we choose the regularization parameter λ properly (and thus control the size of the active set) during the iteration.

In fact, if $\boldsymbol{p}_0 = \boldsymbol{\Phi}\boldsymbol{w}^\star + \boldsymbol{p}_\varepsilon$ with $\|\boldsymbol{w}^\star\|_{l_0} \leq s$, $s \ll n$ and $\boldsymbol{\Phi}$ satisfies a RIP or MIP condition, the algorithm finds the exact nonzero elements of $\boldsymbol{w}^\star$ and converges in finitely many iterations (see Jiao et al's paper [11, Lemma 3.2 and Theorem 3.1]). Moreover, under the assumptions it holds that the active sets in the jth inner satisfy $\mathrm{A}^j \subseteq \mathrm{supp}(\boldsymbol{w}^\star)$, $\forall j$. Observe that the complexity of the algorithm in (5) is mainly to compute $\boldsymbol{d}^j = \boldsymbol{\Phi}^T(\boldsymbol{p_0} - \boldsymbol{\Phi}\boldsymbol{w}^j)$ and the normal equation (5b). The complexity of the former is simply $\mathcal{O}(mn)$. For the normal equation (5b), we notice that there is $|\mathrm{A}^j| \leq s$ as $\mathrm{A}^j \subseteq \mathrm{supp}(\boldsymbol{w}^\star)$. Thus the complexity for solving (5b) will not exceed $\mathcal{O}(s^3 + s^2 n)$. To summarize, the per-iteration complexity of PDASC will not exceed $\mathcal{O}(s^2 n + mn)$ when $s \ll n$. As the algorithm stops in finite iterations, PDASC is super-efficient for sparse recovery problem. This is reflected in the figure 2B and figure 2D that the higher the sparsity s, the more efficient the PDASC algorithm will be.

Discussion about robustness optimization

The robust optimization computes a plan that can mitigate the dosimetric impact in the presence of setup and range uncertainties specified in the robustness settings. In SPArc-original, robustness optimization with range uncertainties and setup uncertainties are implemented in RayStation. The basis for the robust optimization in RayStation is minimax optimization [12], in which the optimization objective functions that have been selected to be robust are considered in the worst case scenario. SPArc-original with robustness optimization have been tested for various disease sites and clinical indications [13,14]. These studies indicated that robustness optimization is the key to proton arc therapy.For evaluation of robustness, dose can be computed for a density perturbation or isocenter shift [15]. One possible way is to consider the stability of perturbation to spot intensity $\boldsymbol{w}$. This will be our future work.

References

[1] Lou Y, Zeng T, Osher S, et al. A weighted difference of anisotropic and isotropic total variation model for image processing. SIAM Journal on Imaging Sciences. 2015;8(3):1798–1823.

[2] You J, Jiao Y, Lu X, et al. A nonconvex model with minimax concave penalty for image restoration. Journal of Scientific Computing. 2019;78(2):1063–1086.

[3] Zhang CH, Huang J. The sparsity and bias of the lasso selection in high-dimensional linear regression. The Annals of Statistics. 2008;36(4):1567–1594.

[4] Blumensath T, Davies ME. Iterative thresholding for sparse approximations. Journal of Fourier Analysis and Applications. 2008;14(5-6):629–654.

[5] Tropp JA, Gilbert AC. Signal recovery from random measurements via orthogonal matching pursuit. IEEE Transactions on information theory. 2007;53(12):4655–4666.

[6] Needell D, Tropp JA. Cosamp: Iterative signal recovery from incomplete and inaccurate samples. Applied and Computational Harmonic Analysis. 2009;26(3):301–321.

[7] Foucart S. Hard thresholding pursuit: an algorithm for compressive sensing. SIAM Journal on Numerical Analysis. 2011;49(6):2543–2563.

[8] Kashin BS, Temlyakov VN. A remark on compressed sensing. Mathematical notes. 2007; 82(5):748–755.

[9] Candes EJ, et al. The restricted isometry property and its implications for compressed sensing. Comptes Rendus Mathematique. 2008;346(9-10):589–592.

[10] Donoho DL, Huo X, et al. Uncertainty principles and ideal atomic decomposition. IEEE transactions on information theory. 2001;47(7):2845–2862.

[11] Jiao Y, Jin B, Lu X. A primal dual active set with continuation algorithm for the 0-regularized optimization problem. Applied and Computational Harmonic Analysis. 2015; 39(3):400–426.

[12] Fredriksson A, Forsgren A, Hårdemark B. Minimax optimization for handling range and setup uncertainties in proton therapy. Medical physics. 2011;38(3):1672–1684.

[13] Li X, Kabolizadeh P, Yan D, et al. Improve dosimetric outcome in stage iii non-small-cell lung cancer treatment using spot-scanning proton arc (sparc) therapy. Radiation Oncology. 2018;13(1):1–9.

[14] Chang S, Liu G, Zhao L, et al. Feasibility study: spot-scanning proton arc therapy (sparc) for left-sided whole breast radiotherapy. Radiation Oncology. 2020;15(1):1–11.

[15] Laboratories R. RayStation 6 user manual. Sweden; 2016. RSL-D-RS-6.0-USM-EN-1.0-2016-12-22.